Tribology Letters (2024) 72:46
https://doi.org/10.1007/s11249-024-01847-3

ORIGINAL PAPER

Enhancing the Elastohydrodynamic Lubrication and Vibration Behavior of Rolling Bearings Using a Hybrid Bio-Grease Blended with Activated Carbon Nanoparticles

Zeyad A. Abouelkasem[1] · Galal A. Nassef[1] · Mohamed Abdelnaeem[2] · Mohamed G. A. Nassef[1,3]

Received: 22 December 2023 / Accepted: 29 February 2024

Abstract
In recent years, bio-lubricants have received a growing interest for industrial applications. Still, a full-scale implementation in machinery lubrication requires a thorough evaluation of their performance through tribological and operational tests to stand upon their performance. Additionally, the promising outcomes achieved by nanoadditives in improving the performance of synthetic lubricants have prompted research efforts to identify suitable nanoadditives for bio-grease. This paper introduces a bio-grease from a hybrid vegetable oil and glycerol monostearate as a thickener for the lubrication of rolling bearings. Activated carbon nanoparticles (ACNPs) as nanoadditives were synthesized, characterized, and incorporated into the bio-grease at concentrations of 0.5, 1, and 2% by weight. Tribo-tests were conducted on these bio-grease blends, and running tests were carried out using 6006 ball bearings on a custom test rig. Throughout a 30-min test run under a radial load of 10% of the bearing's dynamic load rating, mechanical vibrations and power consumption were measured and analyzed for each bearing. The bio-grease with ACNPs exhibited a substantial reduction in wear scar diameter (WSD) and coefficient of friction (COF), achieving improvements of up to 73.6 and 65%, respectively, in comparison to lithium grease. Furthermore, the load carrying capacity was enhanced by 200%. The study revealed a strong correlation between measured vibration amplitudes and the viscosity of the bio-grease. The absence of high frequency resonant bands in vibration spectra indicated that the test grease samples satisfied the conditions of elastohydrodynamic lubrication, and these findings were corroborated through calculations of the minimum oil film thickness.

Keywords Vegetable oil-based grease · Tribology · Activated carbon nanoparticles · Vibration levels · EHL film

1 Introduction

Friction and wear are major contributors to approximately 80% of mechanical failures, which, as per statistics, account for about one-fourth of the world's total energy consumption [1, 2]. Many researchers are striving hard to reduce friction by developing one of the following interacting aspects: lubrication, material, and component design. Lubrication is the key to effective and efficient tribological contact, shifting the lubrication concept from mobility to durability and, most recently to sustainability.

In recent years, bio-lubricants have received a growing interest for industrial applications due to their high sustainability and low impact on the environment [3–5]. Compared to conventional lubricants derived from fossil origin, bio-lubricants are derived from renewable resources such as vegetable oils, animal fats, or even microalgae. This inherent renewable nature makes them particularly attractive.

✉ Mohamed G. A. Nassef
mohamed.nassef@ejust.edu.eg

Zeyad A. Abouelkasem
Zeyad.Abouelkasem@alexu.edu.eg

Galal A. Nassef
galalnassef@alexu.edu.eg

Mohamed Abdelnaeem
m_abdelnaeem_2@alexu.edu.eg

[1] Production Engineering Department, Alexandria University, Alexandria 21544, Egypt

[2] Mechanical Engineering Department, Alexandria University, Alexandria 21544, Egypt

[3] Industrial and Manufacturing Engineering Department, Egypt-Japan University of Science and Technology, New Borg El-Arab City 21934, Egypt

Published online: 01 April 2024

Furthermore, previous research works reported promising thermophysical and tribological performance of bio-lubricants in rotating machinery [6]. In general, vegetable oils exhibit higher lubricity and better wear resistance than commercial mineral oils. They mainly consist of triglyceride that adsorbs to the metal surface due to the polar groups and long fatty acid chain length [7, 8]. However, the concentrations of fatty acids in the oil profile differ depending on the oil source, which is mainly responsible for its properties. Vegetable oils with high mono-unsaturation fatty acids content such as avocado, olive, castor, and jojoba possess excellent oxidative and thermal stability [9, 10]. Sierra et al. [11] investigated the castor oil's tribological properties when applied to a steel surface using a pin-on-disc machine. They compared the obtained results with commercial oil. It has been found that friction coefficient is reduced by 75% when applying castor oil.

Few researchers worldwide have focused on bio-based grease thickener development, with notable efforts involving sorbitan/glyceryl stearate and cellulose/chitin derivatives [12, 13]. Notably, research has demonstrated that biogreases derived from castor oil with glyceryl monostearate as a thickener exhibit lower friction coefficients compared to other natural thickeners and even outperform commercial lithium grease in tribological tests [14, 15]. Given its synthesis as a food-grade emulsifier, glyceryl monostearate offers distinct advantages, including enhanced consistency and yield stress [16, 17], making it a prime candidate for bio-grease thickening. Nonetheless, there remains a need for further research exploring environmentally friendly additives and their interactions with bio-greases to optimize performance [18–20].

The twenty-first century has witnessed a remarkable revolution in nanotechnology, offering a unique avenue for the exploration of various nanomaterials in lubricating oils and greases. A significant aspect of these nanomaterials is their environmentally friendly nature, devoid of sulfur and phosphorus content, making them ideal additives for eco-conscious applications [21]. Nanomaterial additives have been shown to enhance lubricity, reduce friction and wear, improve vibration damping, and enhance load-bearing capacity, thereby contributing to energy conservation [22–24]. These additives are classified based on criteria such as dimensionality, morphology, and chemical composition, with categories encompassing nanometal-based materials (e.g., pure metals, metal oxides, metal salts, metal sulfides, and metal hydroxides), nanocarbon-based materials (including pure carbon and polymers), and nanocomposite-based additives [23, 25]. For example, Padgurskas et al. [26] explored the use of Fe, Cu, and Co nanoparticles as lubricant additives, reporting an average 50% reduction in wear and friction, along with an enhanced load carrying capacity, rendering them suitable for industrial applications. Comprehensive investigations have shed light on the role of nano additives in enhancing tribological performance, including colloidal effects, rolling effects, third-body mechanisms, and the formation of protective films [27].

Compared to other nanoadditives, carbonaceous nanomaterials such as graphene, graphene oxide, and multiwall carbon nanotubes (MWCNT) are seizing the attention because they possess outstanding tribological, electrical, thermal, and chemical properties with eco-friendly advantage for a sustainable bio-grease [23, 28, 29]. Mohamed et al. [30] investigated adding CNTs to lithium grease. Results show that adding 1 wt % reduced coefficient of friction (COF) and wear scar diameter (WSD) by 82 and 63%, respectively. Also, load carrying capacity has increased by about 52%. Other similar studies on adding MWCNT to lithium grease showed enhancement in the tribological performance of grease by reducing friction up to 42% [31]. Another investigation of adding MWCNT and graphene nanosheet to calcium grease reduced friction and WSD by 60 and 70%, respectively [28]. A recent attempt introduced activated carbon nanoparticles (ACNPs) from polymeric waste as a novel nano additive for lithium grease. The tribological tests proved a superior performance of lithium grease with 1 wt % AC by reducing the coefficient of friction (COF) by 83% [32].

An experimental investigation on deep groove ball bearings was conducted by Nassef et al. [33] using different concentrations of reduced graphene oxide in lithium grease. Results showed higher lubricity presented in lower power consumption by 70% when adding graphene up to 2% wt. Additionally, the vibration amplitudes were reduced by 17% while thermography analysis showed a remarkable enhancement in bearing operating temperatures.

Most of previous investigations focused more on developing a partially bio-grease using green base oil with a synthetic thickener. The majority of studied base oils contain large amounts of polyunsaturated fatty acids which cause the lubricants to suffer from low oxidation and thermal stability. On the other hand, using a bio thickener for grease has not yet proven a sufficient consistency under higher mechanical loads or at elevated temperatures. Selecting an appropriate vegetable oil paired with a compatible green thickener is crucial to attain satisfactory lubricant performance in rotating machinery components like rolling bearings. This paper presents the synthesis and performance analysis of a novel bio-grease, from glycerol monostearate as a thickener and a mixture of castor, jojoba, and bitter almond oils as a hybrid base oil. These vegetable oils are well known for possessing high content of monounsaturated acids beside saturated fatty acids and esters. For possible enhancement of the proposed bio-grease properties, (ACNPs) extracted from recycled polyethylene terephthalate (PET) waste were applied as nanoadditives at different weight concentrations.

Physicochemical and tribological tests are conducted on the grease samples to analyze their load carrying capacity, COF, and WSD. The performance of grease samples is also evaluated as lubricants for ball bearings in a customized test rig. The power consumption and mechanical vibrations of the bearings lubricated with bio-grease containing nanoparticles are measured and analyzed. To confirm that the test bearings lubricated with the developed bio-grease will operate in elastohydrodynamic lubrication (EHL) regime at different radial loads, the oil minimum film thickness is calculated using Hamrock-Dowson equation and compared with values from the commercial lithium grease.

2 Materials and Methods

2.1 Synthesis of Bio-Grease

The proposed bio-grease is prepared by adding 85% base oil to 15% glycerol monostearate as a green thickener. Two main criteria were set in this work for the selection of base oil constituents and their concentrations in the hybrid oil. The first criterion was mainly centered around the types of fatty acids/esters in each individual oil. The three selected oils in this work possess a major content of monounsaturated fatty acids which aligns with literature recommendations to achieve enhanced lubricant performance in terms of oxidation stability and lubricity [34]. In this regard, International Standards Organization Viscosity Grade (ISO VG) of industrial lubricants was used as a guideline for reaching the optimum mixture that can satisfy the operation conditions of rolling bearing applications [35]. Another important criterion that was considered during the planning phase was the impact of choosing the individual base oils on the food market. Only nonedible oils were under focus of study to avoid potential debates surrounding food versus fuel [36]. The base oil employed in this study is a mixture of castor oil (233.75 g), jojoba oil (127.5 g), and bitter almond oil (63.75 g), with the respective weights as specified. All constituents are acquired from a local supplier. During the planning of the experimental work, pilot tests were conducted on mixtures of different concentrations from the three selected individual base oils. The kinematic viscosity of the hybrid oil at 40 and 100 °C was measured and compared to those of industrial oils used for rolling bearings. According to review of literature, the recommended ISO VG for ball bearings fall between VG 68 and 100 [37, 38].

The chemical composition of each vegetable oils used in this work are obtained from the local supplier using gas using Ultra GC–MS (Shimadzu, Kyoto, Japan) chromatography (GC) analysis equipped with an electron impact source. The chemical composition of castor oil consists of ricinoleic acid (90%), oleic acid (3.8%), stearic acid (2%), palmitic acid (1%), linolenic acid (3%). The supplier data are found in agreement with results in [39, 40]. The presence of the monounsaturated fatty acid with long chain (C18:1-OH) and hydroxyl groups results in excellent viscosity and adsorption properties. However, the presence of unsaturated fatty acids harms the thermo-oxidation stability of castor oil.

The main constituents of the purchased jojoba oil are eicosenoic acid (72.7%), erucic acid (12.5%), and oleic acid (10.6%). This composition is slightly different from those reported in previous investigations [41, 42] due to the geographic origin of the jojoba seed itself. The dominant presence of monounsaturated fatty esters in jojoba oil composition along with small traces of saturated pentadecanoic acid and palmitic acid implies high oxidation stability levels. Regarding bitter almond oil, the main constituents are found to be oleic acid (73.8%), linoleic acid (17.3%), and palmitic acid (7%). The chemical composition of bitter almond oil from the supplier is found similar to literature data [43].

The preparation process involves initially placing the entire oil mixture into an open vessel. This vessel is then heated to a temperature of 40 °C, and manual stirring is carried out for a duration of 10 min to ensure homogenization of the mixture. Subsequently, glycerol monostearate (75 g) is added to the mixture in the vessel, which is then stirred at 60 rpm. The temperature within the vessel is raised to 80 °C and maintained at this level for a period of 60 min, ensuring the thorough dispersion of the glycerol monostearate within the mixture. Finally, the solution is cooled down to 25 °C by immersing the vessel in a water bath. Figure 1. shows the prepared samples of the bio-grease.

2.2 Synthesis and Mixing of Activated Carbon

Activated carbon (AC) is extracted from plastic bottle waste and synthesized into nano-powder as described in [32]. Polyethylene terephthalate (PET) plastic bottle waste is washed, sun-dried, and shredded. 25 g of the cleaned PET particles are placed in a sealed stainless-steel autoclave, then heated in an electric muffle furnace (ASH AMF 25N) at a rate of 25 °C min^{-1} to 500 °C for one hour. The system is cool for around 12 h. The resulting synthetic activated carbon (AC) is milled with an Electric Grain Spices Multifunctional grinder (ST3-E4842UK), England, for 10 min to sizes below 0.09 µm. In this work, ACNPs are added with 0.5, 1, and 2 wt % to the prepared bio-grease samples. Table 1 shows the type and concentrations of each studied test blend.

2.3 Material Characterization

The nanostructure of the activated carbon nanoparticles (ACNPs) is examined using Scanning Electron Microscopy (SEM) (JEOL JSM-6010LV instrument, Akishima, Tokyo, Japan). The SEM examination is intended to obtain

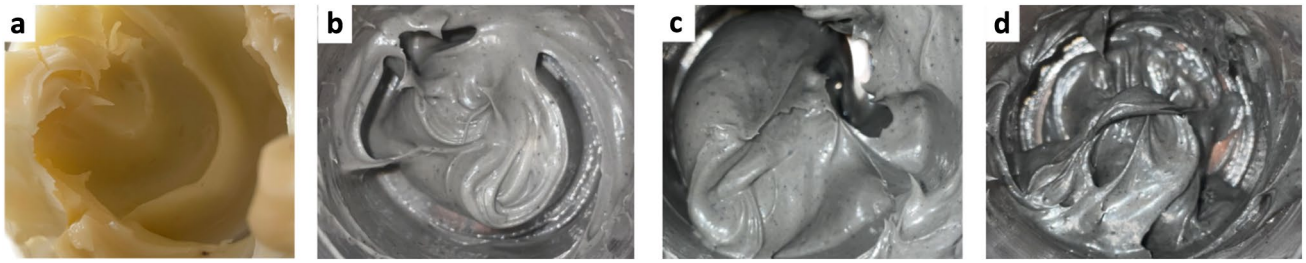

Fig. 1 The photographs of synthesized grease samples: **a** bio-grease without nanoadditives **b** bio-grease with 0.5 wt % ACNPs, **c** bio-grease with 1 wt % ACNPs, **d** bio-grease with 2 wt % ACNPs

Table 1 Proportions (quantities) of additives and the designations of formulated greases

Grease type	Sample	ACNPs concentration
Bio-grease (castor oil, jojoba oil, and bitter almond oil)	CJB	–
	CJB0.5	0.5 wt %
	CJB1	1 wt %
	CJB2	2 wt %
Commercial lithium grease	LG	–

ACNPs particle morphology, size, and composition. The surface area of the activated carbon is quantified using the Brunauer–Emmett–Teller (BET) method. BET method was conducted using Microtrac MRB BELSORP-mini X, BEL Japan operating at a temperature of − 200 °C and equipped with pressure sensors on the ACNPs samples to evaluate the specific surface area of ACNPs material, the pore size distribution, pore volume, and the average pore diameter. The pore size distribution was evaluated using the Barrett–Joyner–Halenda (BJH) model. BELSORP-mini X can evaluate pore size distributions from 0.7 to 500 nm.

FTIR (Fourier Transform Infrared Spectroscopy) spectra analysis is conducted on the ACNPs to identify the most significant functional groups. The analysis is performed within the wavelength range of 400–4000 cm^{-1}, utilizing a Shimadzu FTIR-8400 S instrument (Nakagyo-ku, Kyoto, Japan). Additionally, X-ray diffractometer (XRD) analysis is employed to confirm the purity of the activated carbon. This evaluation involves the utilization of a Shimadzu 7000 Diffractometer that operates with Cu Kα1 radiation (k = 0.15406 nm) generated at 30 kV and 30 mA. The scanning process is conducted at a rate of 2° min^{-1} for 2 theta values ranging from 20° to 80°.

2.4 Kinematic Viscosity Test

The kinematic viscosity of each individual oil sample beside the oil mixture is tested using VSDT-3000 Viscosity Density Meter in accordance with ASTM-D445. The results from testing each oil sample will be used to determine the viscosity index values to determine the oil resistance to change in viscosity at elevated temperatures. In each test, an oily sample of 30 mL is allowed to flow through a capillary viscometer immersed in a liquid bath at 40, 60, 80, and 100 °C temperatures. Then, the kinematic viscosity is calculated in centistokes (cSt) by multiplying the time that the oil takes to pass through the minimum and maximum intervals within the capillary by the viscometer constant.

2.5 Wettability Analysis

One important factor that controls the adsorption and interfacial properties of the vegetable oils is the wettability and surface tension of metallic surface. The oil droplets that tend to spread out over a larger surface area result in a smaller contact angle and hence achieves a good wettability of the surface, while oil droplets tending to form spheres results in large contact angle with the surface and thus have low wettability. For this purpose, wettability test is conducted to the vegetable oil samples using the Krüss EasyDrop (FM40, KRÜSS GmbH, Hamburg, Germany) goniometer device, according to ASTM D7334-08.

The test starts by releasing a 0.3 µL droplet of test the vegetable oil from a syringe to fall under the effect of gravity on a flat and polished AISI 52100 steel surfaces. The image of the stationary oil droplet on the surface is then captured within 30 s using a monochrome interline CCD camera with the assistance of software. The contact angle is determined between the droplet and solid surface.

2.6 Tribological Tests

The tribological assessment of the grease samples was conducted to ascertain the load carrying capacity using a customized tribotester based on Brugger's test method. The Brugger's test apparatus, known for its efficiency in reducing test duration, comprises a crossed-cylinder wear tester. This tribotester setup involves two perpendicularly

oriented cylinders, as illustrated in Fig. 2. The top cylinder, known as the roller, is pressed against the bottom ring which rotates at a specific speed for a predetermined duration or number of revolutions. The roller, with a diameter of 11 mm and a width of 15 mm, interfaces with a ring of 25 mm diameter. Both the roller and ring are manufactured from AISI 52100 steel.

The test sequence begins by introducing eight grams of the lubricant blend between the roller and ring. The motor runs for 30 s without applying load to ensure uniform distribution of the lubricant. Subsequently, a step load of 500 g is added to the lever mechanism, excluding the lever arm weight. The test rig is set to operate at 800 ± 5 revolutions per minute (RPM) for a duration of 10 min $\pm$ 15 s, unless indications of scoring are detected earlier. If any scoring occurs during the test, signified by heightened noise and vibration, the test is promptly stopped, and the load is removed. Post-test assessment involves an examination of the roller surface for any signs of scoring or welding. If none are observed, a new test roller is utilized with an increased load step, and the process is repeated until scoring is detected. The load value that triggers scoring is recorded as a seizure load while the previous load step is considered as the load carrying capacity. This entire procedure is repeated three times to ensure the reliability and consistency of the results.

The WSD and COF of each tested bio-grease sample are assessed as the average value of the individual measurements obtained using four-ball wear test according to ASTM D2266 and ASTM D5183, respectively. The device consists of a top ball (12.7 mm diameter) rotating against three bottom balls in a cup filled with the 10 mL test bio-grease. During the test run, the balls rotate at 1200 ± 60 rpm at a temperature of 75 ± 2 °C under 400 N pressing load on the top ball for 60 ± 1 min. At the end of each test, the three lower balls are examined for wear scar using a microscope to determine the WSD. The average of the three WSD values is recorded for the test grease sample. On the other hand, the COF is determined using a stepwise test using 10 kg load in each step with time interval of 10 min at 600 rpm until reaching the onset of welding/seizure between mating surfaces.

2.7 Bearing Running Test

In the current study, a bearing test setup, shown in Fig. 3 and described in [33], is utilized to investigate the influence of nanoparticle-infused grease on bearing vibrations. Deep groove ball bearings type 6006 DDU are used as the test bearings which is lubricated with a suitable quantity of the test grease blends. The experimental setup involved the application of a motor speed of 1400 rpm and radial load of 200 N on the test bearing.

Vibrations emitted by the test bearing were captured using an accelerometer attached to the housing in both radial vertical and horizontal directions via magnet. The acquired signals underwent processing through anti-aliasing filtering, amplification, and integration. The vibration levels were recorded in terms of velocity (mm/s) root mean square (RMS) values.

3 Results

3.1 Characterization Results of Nanoparticles

Figure 4 illustrates the SEM and TEM micrographs of the ACNPs samples, respectively. The micrograph in Fig. 4a reveals the prepared AC nano-powder, displaying well-defined yet aggregated characteristics, forming a composite of blocky morphologies with varying shapes and sizes. The TEM image (Fig. 4b) shows the AC sheets entangled and rippled. The average particle size of ACNPs is calculated using ImageJ open-source software and was found to be approximately 83 nm.

Table 2 shows information about Brunauer–Emmett–Teller (BET) surface area, total pore volume, and mean diameter of pores. ACNPs exhibits microporous morphology based on classification of the International Union of Pure and Applied Chemistry (IUPAC) [44]. The analysis of the pore distribution of AC

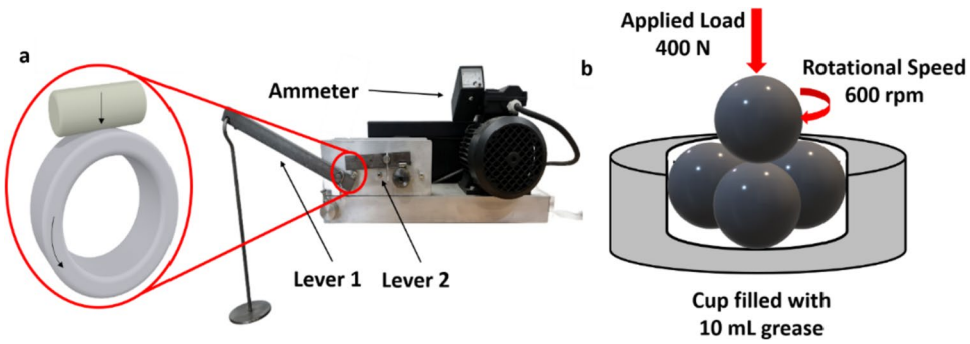

Fig. 2 **a** Customized tribotester based on Brugger's test, **b** Principle of Four-ball tribological test setup

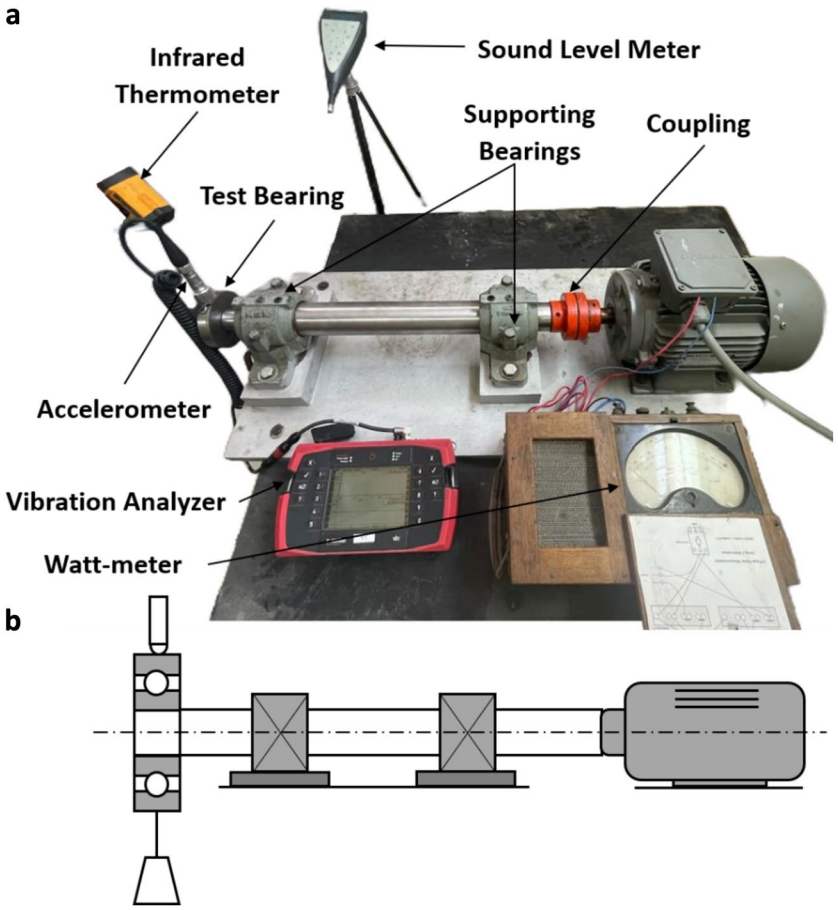

Fig. 3 **a** Bearing Test Setup and **b** Schematic diagram of test setup

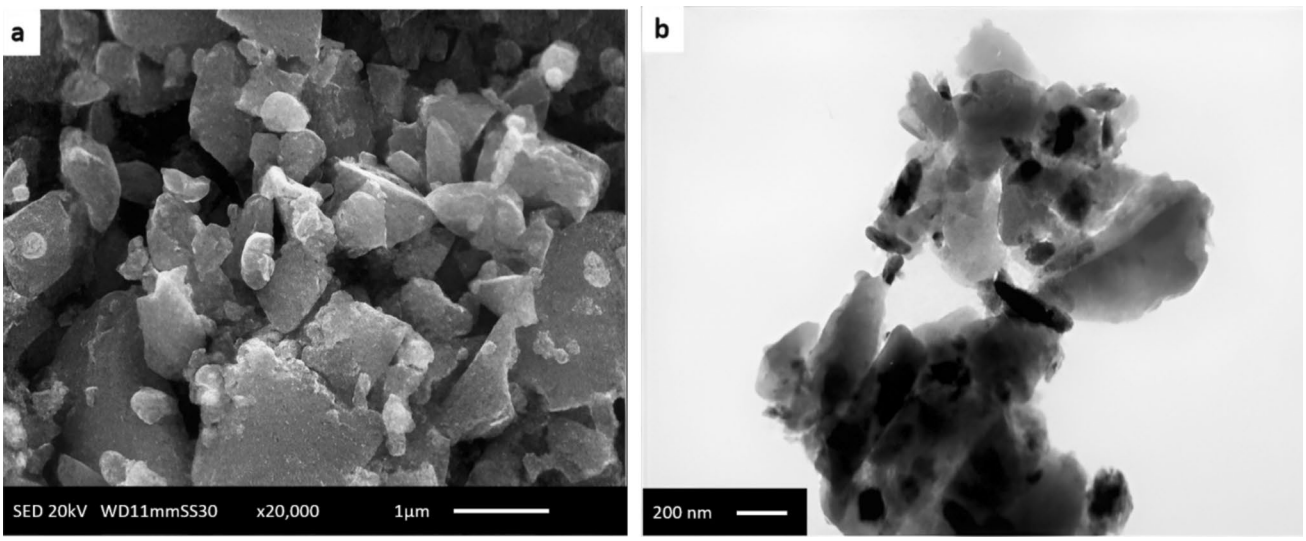

Fig. 4 **a** SEM micrograph, **b** TEM micrograph of ACNPs

verifies the prevalence of micropores with mean pore diameter of approximately 1.8 nm. The considerable volume of larger pores identified within the AC nano-powder can be attributed to the agglomeration of individual pores as a result of arrangement of carbon layers [45]. Heating the char to 500 °C activates both its surface and interior. This activation happens because of the presence of abundant hydrocarbon radicals, along with some hydrogen and water vapor. As a

Table 2 BET surface area, total pore volume, and mean pore diameter and of ACNP

Sample	BET surface area	Total pore volume	Mean pore diameter
AC	448.88 m^2g^{-1}	0.2029 cm^3g^{-1}	1.8080 nm

result, the produced AC becomes amorphous in nature, possesses a high pore volume, and exhibits a large surface area [46, 47].

XRD profile of AC nano-powder is shown in Fig. 5a. The broad diffraction band at 2θ between 20° and 30°, the second feature is a weak intensity peak at 2θ value of 43.2° corresponds to reflections (002) and (101), respectively. The appearance of these bands indicates that AC possesses structures that lie between crystalline graphitic and amorphous states. This type of structure is often referred to as the turbostratic structure or random layer lattice structure [48, 49]. The small peak close to 35° is attributed to an amorphous structure that was irregularly stacked by carbon rings; these rings are not neatly stacked, creating a highly porous and disordered structure. These gaps act as adsorption sites, attracting and holding various molecules on their surfaces. Raman spectrum of AC is used to investigate carbon microstructure (Fig. 5b) and show two intense peak allocated at 1348 and 1590 cm^{-1} corresponding to disordered (D) and graphitic (G) band, respectively. The D band is not present in materials with a high degree of crystallinity, so its presence is due to lattice defects and edge imperfection. Meanwhile G band is related to in-plane stretching vibration of C=C in sp2. Moreover, two more weak peaks were presented at 2680 and 2844 cm^{-1} which could be attributed to the overtone of carbon, suggesting the existence of a carbon material with a few layers [48, 50].

Figure 6 shows the FTIR spectrum which presents the functional groups of AC. Firstly, a broad band at 3421.62 cm^{-1} is attributed to O–H stretching vibration from hydrogen bond of polymeric compounds alcohols, carboxylic acids, phenols, and lattice water [51]. The peak at 1572.49 cm^{-1} is due to skeletal C=C stretching of graphitic carbon's aromatic rings [51, 52]. A sharp peak of medium intensity at 1177.33 cm^{-1} is due to epoxy group C-O vibrations. Finally, the peak at 506.27 cm^{-1} results from out-of-plane angular deformation of AC aromatic rings [53].

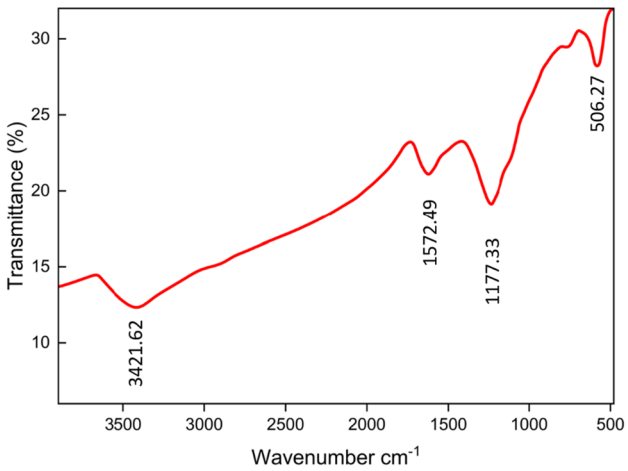

Fig. 6 FTIR spectra of the synthetic ACNPs

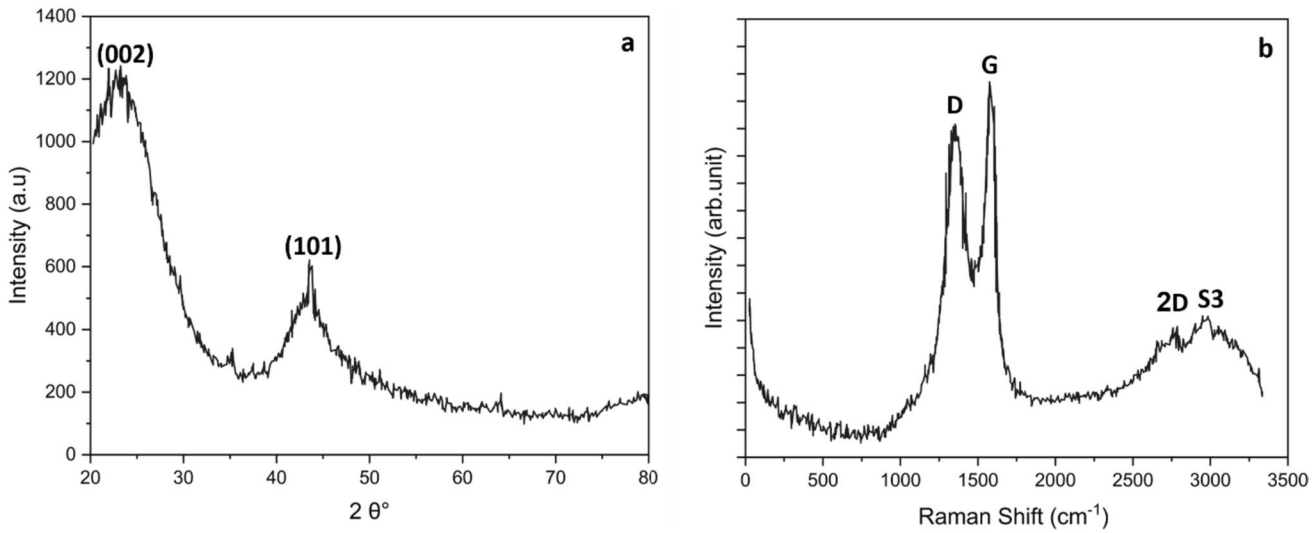

Fig. 5 **a** XRD pattern and **b** Raman spectrum of synthesized ACNPs

3.2 Kinematic Viscosity Results

The kinematic viscosity values of the bio-grease samples at 40, 60, 80, and 100 °C are illustrated in Fig. 7. Castor oil shows the highest kinematic viscosity values of 226.68 mm^2 s^{-1} at 40 °C while jojoba oil and bitter almond oil exhibit the lowest values of only 33.43 and 34.52 mm^2 s^{-1}, respectively. The difference in kinematic viscosity of the vegetable oils is greatly influenced by the length of the carbon chains and the degree of saturation of the fatty acids. The high kinematic viscosity of castor oil is primarily attributed to its unique fatty acid composition. Castor oil is rich in ricinoleic acid, which is a hydroxy fatty acid with a hydroxyl (–OH) group attached to the 12th carbon of the fatty acid chain. Ricinoleic acid has a relatively large and polar structure due to the hydroxyl group, making it less prone to close packing and resulting in a bulkier molecule. The presence of these large and polar molecules in castor oil increases the intermolecular forces and reduces the fluidity of the oil, leading to higher viscosity [40, 54]. Unlike traditional oils, jojoba oil has a lower viscosity due to the absence of triglycerides and the presence of 95% long chain wax esters. The molecular structure of these long straight-chain esters results in a more fluid and less viscous nature [41, 55, 56]. However, this reflected on higher VI of jojoba oil (217) is than that of castor oil (117). Hence, jojoba oil has a higher consistency at fluctuating temperatures than castor oil.

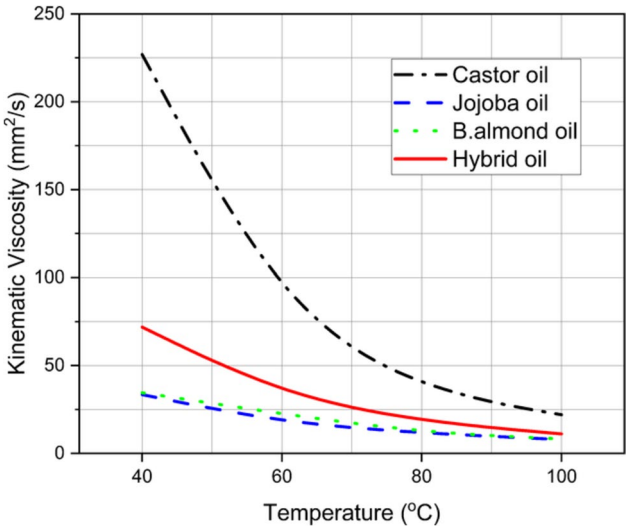

Fig. 7 Kinematic viscosity of the individual oils and the hybrid base oil

The kinematic viscosity of bitter almond oil is found similar to jojoba oil and much lower than castor oil. Bitter almond oil as showed previously having a relatively high concentration of unsaturated fatty acids, such as oleic acid. Unsaturated fatty acids have fewer carbon-hydrogen bonds compared to saturated fatty acids, leading to a more fluid and less viscous nature. Additionally, bitter almond oil may contain a significant amount of monounsaturated fats, contributing to its lower viscosity [43, 57].

As a result of each individual oil properties and concentration, the hybrid oil exhibits kinematic viscosities of 72 and 11.12 mm^2 s^{-1} at 40 and 100 °C, respectively. The oil also shows a high VI of 146. According to ISO 3448, the viscosity of the hybrid oil is found equivalent to viscosity grade ISO VG 68 which promotes it to be classified as an industrial lubricant.

A comparative study between SAE 40 mineral oil and sunflower oil for engine lubrication was conducted in [58]. The outcomes of the analysis showed that kinematic viscosities of the mineral oil are 54.15 and 12.14 cSt at 40 and 100 °C, while the vegetable oil had 46.15 and 10.80 cSt at 40 and 100 °C, respectively. In the current study, hybrid oil exhibits higher kinematic viscosity by 33 and 56% than the SAE40 and sunflower oil, respectively.

3.3 Wettability and Surface Tension Results

Figure 8 displays the calculated contact angle (CA) of the three mixed oils as well as the hybrid oil. It can be seen that castor oil has the largest contact angle of 42.27° while bitter almond oil shows the lowest CA value (18.86°). The physical adsorption between hybrid oil and the contact surface is manifested by a smaller CA (25.28°) than castor oil and

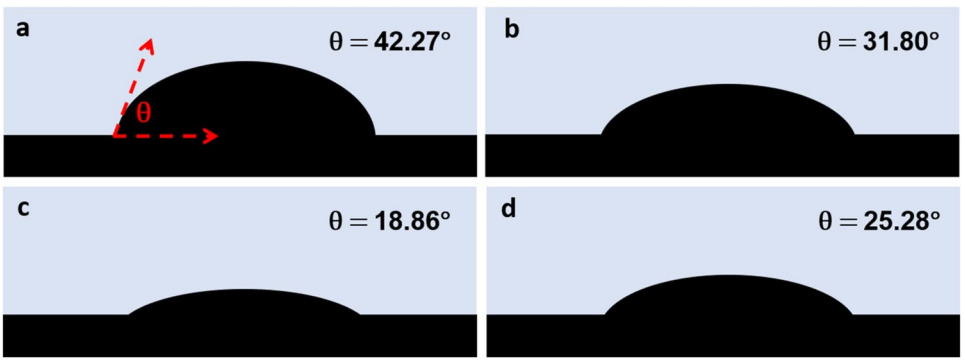

Fig. 8 Contact angle for: **a** castor oil, **b** jojoba oil, **c** bitter almond oil, and **d** hybrid oil

jojoba oil which indicates high wettability on the mating surface and better lubrication of the surface. The differences in contact angle values between the individual oils is mainly attributed to the kinematic viscosity which influences the surface tension between lubricant and metal surface [59]. Table 3 shows the surface tension values for each oil type along with the CA values. It can be seen that the surface tension of oil droplets is proportional to the CA of each oil. Surface tension is the controlling factor of the wettability of oil on the surface, hence the lubricating efficiency. The surface tension is the force acting on the surface layer of the oil droplet in the liquid/gas interface which causes the oil molecules on interface to contract inwards. The surface tension of vegetable oil is controlled by the kinematic viscosity. Fatty acids and esters with long hydrocarbon chains results in a large intermolecular force, hence, high viscosity and higher surface tension [60, 61]. In the case of castor oil, ricinoleic fatty acid (C18H34O3) is the major constituent while 11-eicosenoic acid (C20H38O2) is the main monounsaturated fatty acid in jojoba oil. On the other hand, oleic acid (C18H34O2) and minor content of linoleic acid represents the chemical composition of bitter almond oil. Ricinoleic acid has relatively stronger molecular interaction forces in comparison with the rest of the similar unsaturated fatty acids thanks to its hydroxyl group, enabling hydrogen bonding which is absent in most saturated fatty acids. Furthermore, ricinoleic acid possesses longer chain length, and one double bond that contributes to its strong intermolecular interactions. Hence, castor oil possesses the highest kinematic viscosity which leads to the highest surface tension, largest contact angle, and lowest wettability. In the case of jojoba oil, 11-eicosenoic acid has lower intermolecular forces in comparison with castor oil, hence, it has lower viscosity and higher wettability. The Bitter almond oil consists of a large amount of oleic acid (C18H34O2) and some content of linoleic acid (C18H32O2) as polyunsaturated fatty acid which results in the smallest kinematic viscosity and highest wettability. Hence, the developed hybrid oil shows excellent wettability levels with an acceptable compromise of kinematic viscosity values.

In Ref. [62], the wettability of palm oil (PO) with and without graphene nanoplatelets (GNPs) were evaluated in comparison with commercial cutting fluids for grinding operations. The CA of the commercially cutting fluid was found to be 26.23° while the CA of PO was around 22.15°. In comparison, the CA results of hybrid oil 25.28° which is slightly lower than the commercial cutting fluid and higher by around 12%. In another work [63], the wetting characteristics of a commercially available cutting fluid of BLASER Vasco 6000 (VB 6000) were defined by a CA of 27° while rapeseed oil exhibited better wettability of 24°. The CA values in case of CJB oil were found lower than the VB6000 fluid by 7% and around the same value of rapeseed oil used as cutting fluid.

Table 3 Surface tension measured values for each oil type

Oil	Surface tension (mN/m)
Castor oil	38.8
Jojoba oil	31.4
Bitter almond oil	24.8
Hybrid oil	28.2

3.4 Tribological Performance Results

Extreme pressure (EP) performance of greases is characterized by the non-seizure load. The higher the seizure load is, the higher is the capability of grease to resist adhesion and rubbing of the two mating surfaces. As shown in Fig. 7. the developed bio-grease shows in general lower load carrying capacity than lithium grease. The addition of ACNPs to the developed grease at low concentrations (0.5 wt % ACNPs) showed insignificant changes in load carrying capacity. Increasing the ACNPs weight percentage in the grease blend to 1 wt % led to 66% enhancement in EP properties. A maximum improvement of 200% in load carrying capacity has been reported for grease samples containing 2 wt %.

All the tested bio-grease samples showed a better tribological performance compared to commercial lithium grease. The COF of bio-grease containing 1 wt % ACNPs is lower by around 68% than that of lithium grease. A further increase of ANCPs concentration beyond 1 wt % leads to an increase in the COF.

The results of WSD for all bio-grease samples are plotted in Fig. 8b. The average WSD for the plain bio-grease was found to be 0.550 mm, which is lower than that of lithium grease. The addition of ACNPs to bio-grease showed a considerable reduction in WSD by 9.1, 55.5, and 73.6% for samples containing 0.5, 1, and 2 wt % compared to bio-grease, respectively. The enhancement of antiwear performance is attributed to the rolling action played by the ACNPs at the pairing surfaces [64].

The results of this work are compared with other grease types from review of literature. Acar et. al. [19] tested different synthetic and biogenic greases for COF and wear scar volume. Synthetic Ester Lithium/Calcium Soap grease and high oleic sunflower oil Lithium-12-hydroxystearate grease shows COF values of 0.08 and 0.1 which are found higher than CJB grease (without ACNPs) by 14 and 43%, respectively. Bio-grease samples from high oleic sunflower oil with Lignosulfonate, Castor Oil with Lignin/polyethylene glycol diglycidyl ether (weight ratio of 1/0.25), and Castor Oil with Lignin/hexamethylene diisocyanate are found to show similar COF values as CJB grease. In another work, Amiruddin et. al. [65] have developed and

tested different bio-grease samples from neem, castor and jatropha bas oils with thickeners from beeswax and hexagonal boron nitride (hBN) nano additives. It was found that grease samples from neem base oil with 5 wt % hBN and castor base oil with 5 wt % hBN results in COF of 0.08 which is higher than CJB0.5, CJB1, and CJB2 by 10% up to 42%. This proves higher efficiency of ACNPs over hBN in reducing friction coefficient.

In Ref. [66], polyurethane oleogels from castor oil and cellulose pulp thickener were developed by biological treatment of agricultural wheat and barley straw residues. The oleogel samples reached COF values in the range between 0.077 and 0.108 which are found to be similar to CJB (Without ACNPs) and higher than CJB1 (with 1 wt % ACNPs) by 37–80%. Regarding WSD results, it was found that oleogel samples with highest glucose accomplished the lowest wear scar size in the range between 0.161 and 0.286 mm in comparison, CJB1 and CJB2 have similar WSD results of 0.25 and 0.145, respectively.

Gallego et al. [67] fabricated three different biopolymer-based greases samples from castor oil as base oil with methylcellulose thickener (MC), chitin thickener (CH), and cellulosic pulp (CP) thickeners. From tribological tests at 400 rpm and 25 °C, the COF results for MC and CH are 0.05, 0.08. These values are found similar to values obtained from CJB1, CJB, respectively. On the other hand, The COF and WSD for CP are 0.125 and 0.8 mm which is higher than CJB (without ACNPs) by around 65% (Fig. 9).

3.5 Bearing Performance Results

The power consumption due to friction was measured for the test bearings lubricated with samples of bio-grease blends under three selected loads (100, 800, and 1800 N), as shown in Fig. 10a. CJB sample (bio-grease without ACNPs) shows slightly lower friction power as compared to LG (lithium grease) at 100 and 800 N. The addition of ACNPs in CJB0.5, CJB1, and CJB2 samples reduced the power loss by amounts ranging from 7 to 17% at 100 and 800 N. An insignificant change in power loss is noticed at 1800 N, as shown in Fig. 10a.

Grease viscoelastic properties play a key role in rolling bearing vibration performance which is considered in previous works as a critical indicator of bearing life and reliability [68, 69]. The measured vibration signals for test bearings are recorded in time and frequency domains and their RMS velocity values are summarized in Fig. 10b. Considering the fact that the acquired vibrations from the bearing seat is a superposition of signal components from various sources, including slight unbalance, background noise, as well as friction occurring between the bearing's raceway and roller at high frequency bands between 900 and 1600 Hz [70, 71]. For all tested bearings, the vibration RMS values are found below the maximum allowable levels according to ISO 10816. Besides, there was no evidence of sharp vibration peaks at HF bands indicating formation of efficient tribofilm layer separating the two mating surfaces. LG and CJB grease samples resulted in similar RMS vibration

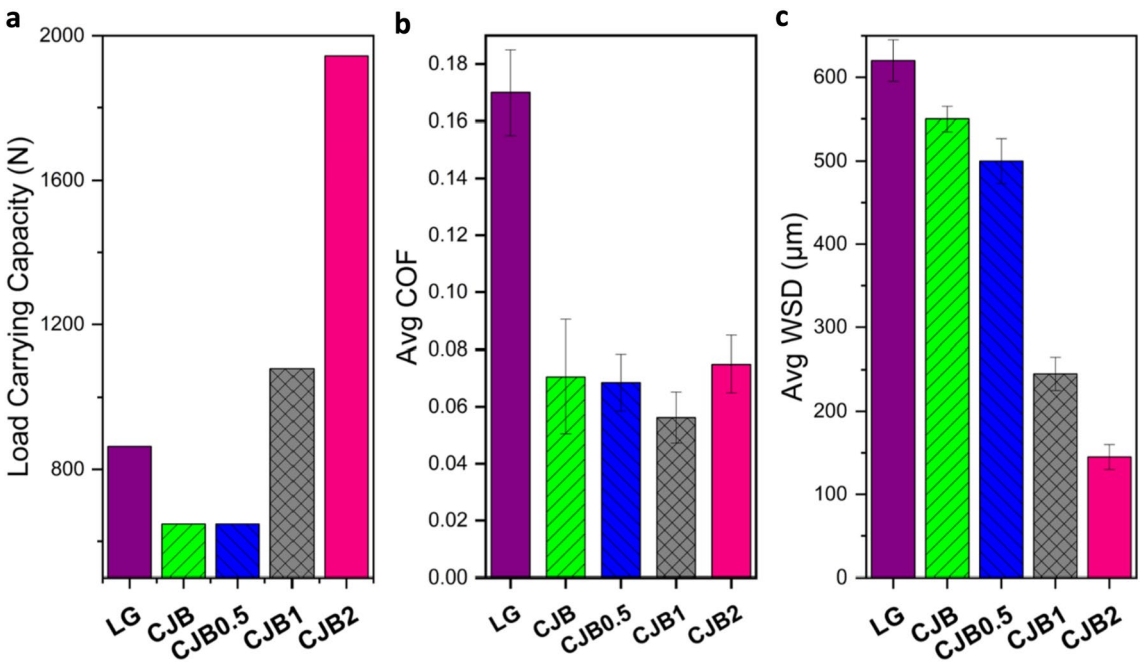

Fig. 9 **a** Load carrying capacity (Non-seizure Load) values for grease samples, **b** Average COF, and **c** average WSD values for grease samples

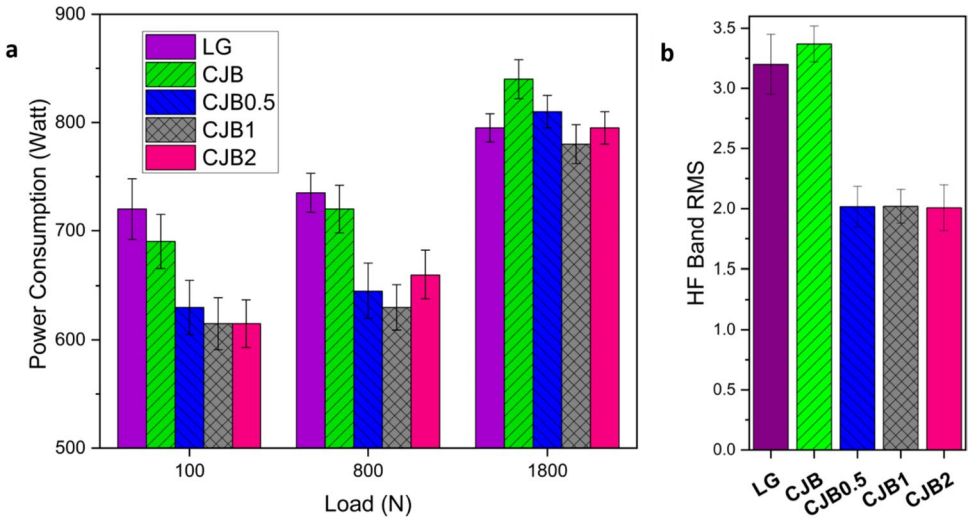

Fig. 10 **a** Power consumption of grease samples at different loads, and **b** HF band RMS values of bearing vibration for grease samples

levels while bearings lubricated with CJB0.5, CJB1, and CJB2 show a considerably lower vibration levels by 85%, in comparison with LG samples. This can be attributed to the high elasticity and damping properties of the carbonaceous nanoparticles [72, 73].

4 Discussion

The developed bio-grease demonstrates remarkable physical, tribological, and dynamic performance, primarily influenced by the long carbon chain length and viscosity of each constituent in the hybrid base oil. The base bio-oil comprises three constituent oils with long fatty acid chains structure of high polarity. This is particularly due to the presence of high ricinoleic acid content in castor oil. This acid serves as an effective antiwear agent, particularly when incorporated into grease [74], owing to its longer hydrocarbon chains with unsaturated bonds [75]. The inherent polarity of hydroxyl and carboxylic groups in the applied bio-lubricants, especially in ricinoleic acid, facilitates their adsorption onto the metal surface, forming a protective tribofilm. Furthermore, this polarity induces the re-orientation and alignment of oil molecules, enhancing the wettability of the bio-oil. This, in turn, ensures efficient coverage of the metallic surface with the tribofilm, thereby maintaining a low COF [76]. Another contributor to the formation of a tribofilm layer and reducing wear scar in comparison with commercial grease is the presence of a large quantity of wax esters in jojoba oil which are easily released from the thickener under the effect of contact pressure within the contact area and adhere to the metallic surfaces. In addition, bitter almond oil plays its part with supplying the contact surface with its monounsaturated long chain oleic acid as its major constituent leading to a good fluidity of the hybrid oil and better wettability.

Nevertheless, the unmodified vegetable oil-based grease sample, despite exhibiting improved tribological performance, remains weak to endure severe wear conditions or high applied loads [77]. This limitation is attributed to the absence of effective antiwear agents in its composition [63, 78].

Hence, the introduction of ACNPs aims to overcome the limitations of the plain bio-grease. ACNPs, characterized by their high surface area and porous structure, possess the ability to cover a larger metallic surface by forming a robust tribofilm, as shown in Fig. 11. This effect was confirmed by Nassef et al. [32] in their investigation about adding ACNPs to lithium grease. They found that the ACNPs were deposited on the metal surface better than graphene nanoadditive due to the porous nature of the ACNPs. Furthermore, ACNPs have a high surface area, creating numerous opportunities for intermolecular interactions with surrounding

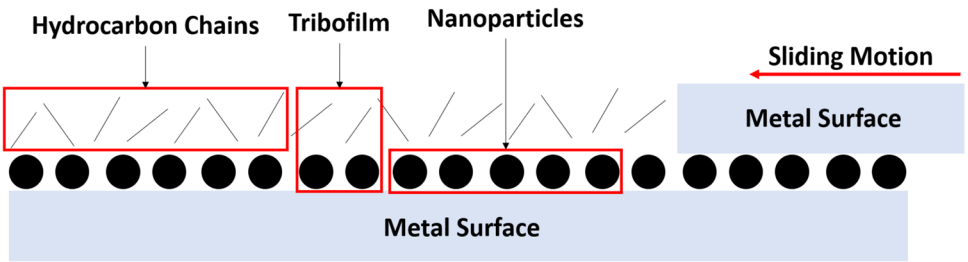

Fig. 11 Effect of Hydrocarbon chains with polar groups and ACNPs on reducing friction during sliding action between metallic surfaces

molecules. Bio-oils, with their complex mixture of polar and nonpolar components, provide diverse interaction sites. There are different possibilities for interactions such as Hydrogen bonding or π-π bonding or Van der Waals bonding forces or hydrophobic interaction between nonpolar regions of nanoparticles and bio-oil molecules [79, 80]. These interactions may contribute to a considerable increase in the viscosity of the bio-oil, primarily attributed to the increased resistance to motion within the oil molecular structure. This viscosity increment results in the formation of a cohesive and more stable tribofilm, which can lead to enhance load carrying capacity.

Figure 12 presents SEM images of the worn-out surfaces lubricated by the developed grease blended with ACNPs. In each image, the arrow indicates the sliding direction, serving as a crucial feature for investigating the worn surface. In Fig. 12a, severe surface damage and plastic deformation are evident, suggesting significant adhesive wear due to the failure of the grease film in a "stick–slip" status at the seizure load during Brugger's test. The addition of ACNPs mitigates the severity of the damage, with deep grooves reduced to some extent. Additionally, abrasive wear is indicated by parallel grooves in Fig. 12b, which could be attributed to altering some sliding motion into rolling motion as nanoparticles influence tribofilm formation. In Fig. 12c and d, an increase in ACNPs concentration enhances the antiwear behavior of the developed grease, significantly reducing wear between rubbing surfaces and resulting in a smoother scar surface. The formulated tribofilm reduces asperity-to-asperity contact, and the higher concentration of ACNPs creates a denser monolayer that effectively protects the mating surfaces from tribo-stress, as found in load carrying capacity results.

To further justify the SEM micrographs for the worn surfaces, Energy Dispersive X-ray (EDX) analysis of the worn surfaces is conducted using (JEOL JSM-IT200, Japan). Figure 13. illustrates the Energy Dispersive X-ray (EDX)

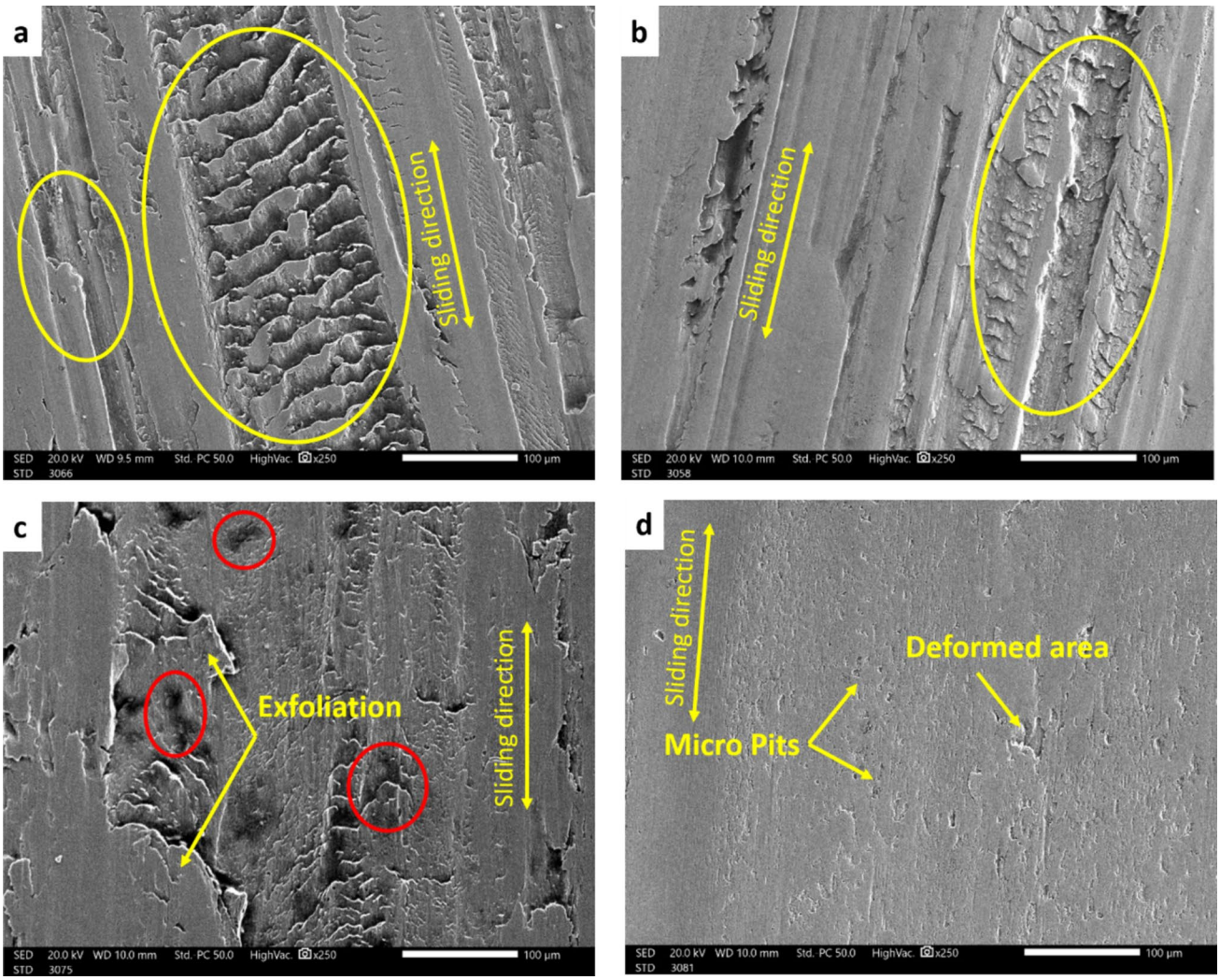

Fig. 12 SEM micrographs of the worn surfaces lubricated with **a** CJB, **b** CJB0.5, **c** CJB1, and **d** CJB2

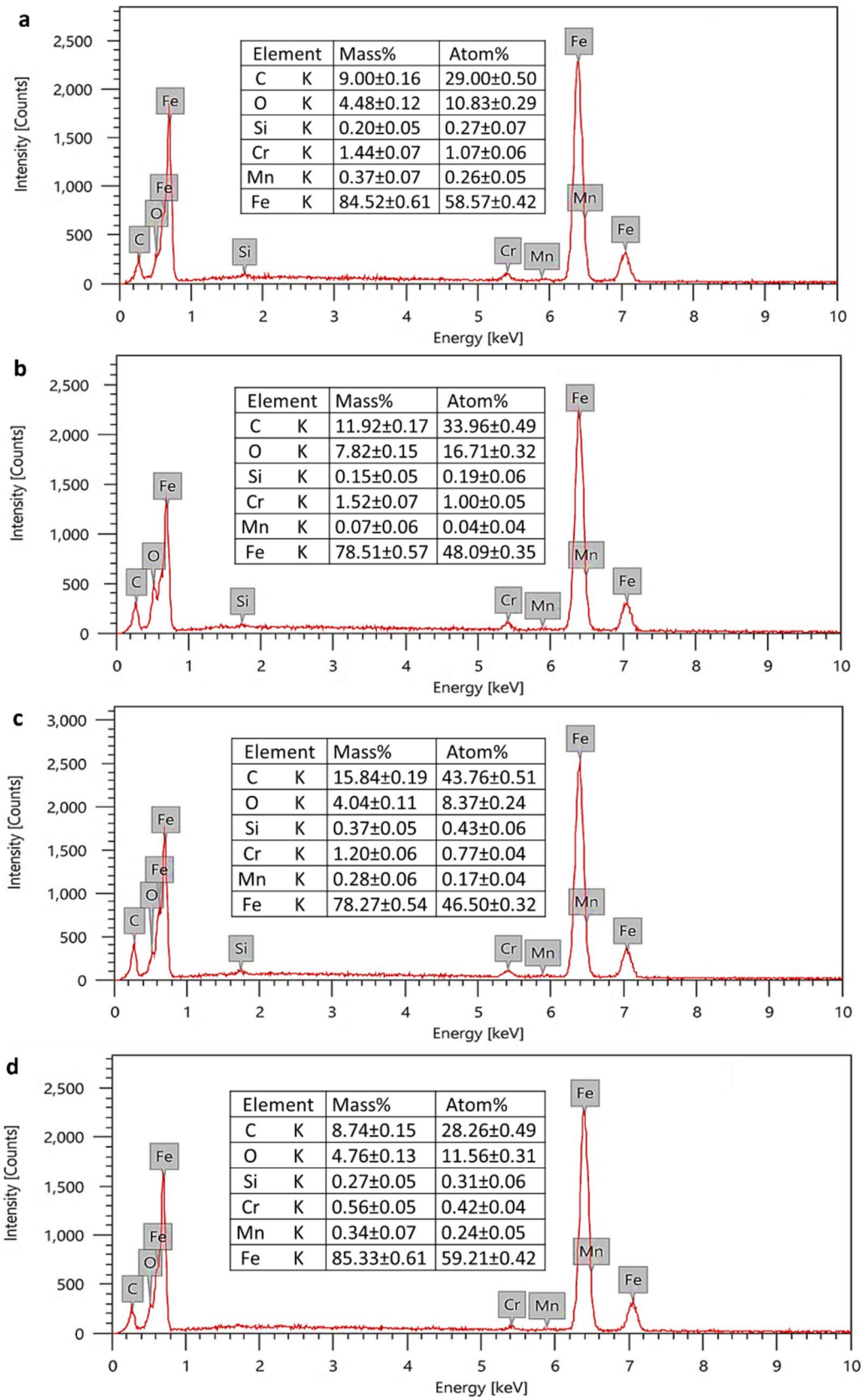

Fig. 13 Typical EDS spectra of worn steel balls lubricated with **a** CJB **b** CJB0.5 **c** CJB1 **d** CJB2

patterns, displaying the elemental content of the tested samples from Brugger's test. In all figures, the results confirm the existence of large content of carbon at 29% and small traces of oxygen at 10.44%. the presence of carbon (C) and oxygen (O) element on the worn surface of the steel cylinder lubricated with test grease samples suggests the existence of the fatty acid constituents from the vegetable oil mixture as an adhered film on the rubbed steel surface, mitigating friction and wear to a certain extent.

The introduction of ACNPs into the developed grease has led to the creation of a more robust absorption layer, providing protection to the contact surfaces. The adsorption layer's formation stems from the interplay between the grease's base oil and ACNPs, influenced by their respective polarities. Increasing the wt % of ACNPs exhibited an improved ability to adhere to the metal surface, leading to the formation of more stable films up to the optimum level. This is supported by the observation of the highest carbon (C) element deposition at the worn areas in Fig. 13c. As per Ref. [81], it is suggested that ACNPs create a chemical monolayer on the metallic surface. Additionally, a physical film of ACNPs is formed above the chemical layer under conditions of heat and high contact pressure. Moreover, this physical film's strength depends on the density of ACNPs, below 2 wt % this layer is failed which interprets the findings of the extraordinary performance of EP property in case of CJB2. Additionally, the physiosorbed layer exhibits a higher COF than the chemical monolayer, indicating that CJB2 displays a higher COF than other blended greases.

During operation, the lubrication of rolling bearings can take place in different lubrication regimes: boundary lubrication, mixed film, or full film lubrication. The contact area between rolling elements and raceway has a high contact pressure and low degree of conformity, i.e., they are classified as non-conformal surfaces. Hence, the full film lubrication is called elastohydrodynamic lubrication (EHL) [82]. According to Vencl et al. [83], oil type and viscosity plays a major role in preserving the formation of a stable elastohydrodynamic lubricating (EHL) film and maintaining no asperity contact. If the lubricant viscosity is insufficient, EHL film will fail to form at the Hertzian contact zone (i.e., lubricant starvation case) [84]. In consequence, an adhesion wear will gradually occur where surface asperities will weld together and eventually break apart leading to formation of localized faults such as micro-pits and abrasive particles that accelerate abrasive wear mechanism [85–87]. Harris [85], lubricant deficiency is considered as one of the main failure causes of rolling bearings with a share up to 80% among other causes.

According to previous findings in Ref. [87], the vibration signal components corresponding to insufficient lubricating conditions between rolling elements and raceways are characterized by high frequency resonant peaks in the range between 900 to 1600 Hz. This is due to rubbing action between surface asperities during operation. Jakubek et al. [88] found that the increase in viscosity of the lubricant will not only reduce broadband vibration levels but also will obscure the vibration signal components included by surface roughness and waviness. Furthermore, Serrato et al. [89], proved that different lubricant viscosity grades affect the vibration response of rolling bearings and the lubrication regime. Oils with high viscosities results in full EHL film and low RMS vibration levels due to low COF between mating surfaces. This is due to the proportional relationship between the oil viscosity grade and the minimum oil film thickness and stiffness [90].

To further understand the influence of the developed grease with the hybrid oil on the obtained vibration levels and power consumption results, the minimum oil film thickness (h_{min}) is calculated. The most common equation to calculate the minimum film thickness in oil-lubricated rolling bearing is Hamrock-Dowson equation [91] as shown in (Eq. 1):

$$H_{min} = 3.63.U^{0.67}.G^{0.49} \cdot W^{-0.073}\left(1 - e^{-0.68.k}\right) \quad (1)$$

where U is speed parameter, G is material parameter and W is loading parameter.

Cen et al. [92–94] investigated correction factor of Hamrock-Dowson equation when applied with grease-lubricated rolling element, observed that the actual minimum film thickness is lower than calculated in case of low speed (< 500 rpm) or before starvation, and higher if operated at higher speed after starvation. In this work, the bearing was sealed and operated at medium speed before starvation.

The λ parameter (Eq. 2), denoting the ratio of the oil film thickness to the surface roughness composite of mating surfaces, is determined to identify the lubrication regime of the operating grease.

$$\lambda = \frac{h_{min}}{\sqrt{{R_{q1}}^2 + {R_{q2}}^2}} \quad (2)$$

where R_{q1} and R_{q1} are the surface roughness values of the rolling element and the inner or outer raceway in contact. If λ values are above 3, then the rolling bearing operated in EHL regime zone. However, λ values between 1 and 3 indicates an operation of bearing in mixed lubrication regime. For values below l, boundary lubrication.

From Eqs. 1 and 2, h_{min} and λ value are calculated for the hybrid oil and the results are summarized in Table 4. The calculated λ parameter for outer and inner race ways are 6.8 and 5.8, shows that minimum film thickness is greater than three times of surface roughness composite of ball bearing [95]. Additionally, metal-to-metal contact is not observed due to the absence of resonant peaks at high frequency zones

Table 4 Calculated minimum oil film thickness and λ parameter for the bio-grease (without additives) at 100 N and 200 N radial loads

Grease type	Bearing load	Bearing raceway	Minimum oil film thickness	λ
Developed bio-grease	100	Inner	0.266	5.80
		Outer	0.313	6.84
	200	Inner	0.253	5.52
		Outer	0.298	6.51
Commercial grease	100	Inner	0.154	3.36
		Outer	0.182	3.79
	200	Inner	0.147	3.20
		Outer	0.173	3.78

which approve that bearing is running in full film condition. Increasing the radial load from 100 to 200 N resulted in a slight reduction in the film thickness. This indicates the ability of the hybrid oil in the grease samples to develop a stable EHL film during the operation of rolling bearing at the two tested radial loads. Furthermore, the calculated h_{min} values in case of the developed bio-grease are found higher than h_{min} values for the commercial lithium grease used in comparison. For instance, h_{min}.

5 Conclusions

In this study, a novel bio-grease formulation was developed for rotating machinery lubrication such as rolling bearings and gears, leveraging a hybrid base oil strategy to enhance lubricity by incorporating monounsaturated oils. This innovative approach not only addresses lubricity but also considers the viscosity profile of the hybrid oil. To further augment its performance and contribute to environmental sustainability, carbonaceous nanoadditives derived from recycled water bottles were introduced, offering a solution to manage non-degradable waste. Specifically, activated carbon nanoparticles (ACNPs) were integrated into the bio-grease as extreme pressure additives, demonstrating an effective strategy to mitigate friction and wear in rolling bearing operations, thereby promoting energy conservation. The following conclusions can be drawn:

- The morphology of the worn surfaces of rollers indicates that a protective film formation on the worn surfaces takes the form of a physisorbed layer created over the chemisorbed layer. The physisorbed layer with a suitable concentration of ACNPs is responsible for the EP behaviour of ACNPs.
- The bio-grease formulations, namely CJB1 and CJB2, exhibited a remarkable reduction in both friction coefficient and average wear scar diameter by 67 and 77%, respectively, when compared to the commercial lithium grease. A corresponding percentage improvement in load carrying capacity for CJB1 and CJB2 was found to be around 25 and 125% in comparison with lithium grease.
- While the bio-grease samples without additives (CJB) showed slightly higher vibration levels than lithium grease, the addition of ACNPs in CJB0.5, CJB1, CJB2 reduced the high frequency vibration of bearings by around 85%. The contact angle values of the hybrid base oil has lower values than castor oil and jojoba oil by 40 and 20%, respectively. This indicates better wettability, which makes the base oil provide the most sufficient supply to the center of the raceway and provide good damping for the contact area so as to reduce the bearing vibration.
- The frictional power losses were reduced by 7–17% for the bio-grease with ACNPs at 100 and 800 N, as compared with the commercial grease. This could lead to improved performance and energy conservation in mechanical systems.
- The calculated h_{min} and λ values for bio-grease indicates the formation of a stable tribofilm layers which are higher by around 68–72% than the values caused by commercial lithium grease. The results ensures that the ball bearings operate within the EHL regime when tested under two different radial loads. This is also confirmed by the absence of high frequency band vibration peaks during vibration analysis of ball bearings indicating the absence of boundary lubrication case.

Acknowledgements The authors declare that no external funds, grants, or other support are received during the preparation of this manuscript.

Author Contributions All authors contributed to the study conception and design. The methodology was planned by Zeyad A. Abouelkasem and Galal A Nassef. Material preparation, data collection and analysis were performed by Zeyad A. Abouelkasem, Galal A Nassef, and Mohamed G A Nassef. The formal analysis and validation of results were performed by Zeyad A. Abouelkasem and Mohamed G A Nassef. The experimental investigation was conducted by Zeyad A. Abouelkasem and Mohamed G A Nassef. The first draft of the manuscript was written by Zeyad A. Abouelkasem. Writing-review and

editing were performed by Mohamed G A Nassef and Galal A Nassef and Mohamed Abdelnaeem. All authors have read and agreed to the final version of the manuscript.

Funding Open access funding provided by The Science, Technology & Innovation Funding Authority (STDF) in cooperation with The Egyptian Knowledge Bank (EKB). The authors declare that no funds, grants, or other support were received during the preparation of this manuscript.

Data Availability The data that support the findings of this manuscript are available from the corresponding author upon request.

Declarations

Conflicts of interest The authors declare that they have no known competing financial interests or personal relationships that could have appeared to influence the work reported in this paper.

Ethical Approval No ethical approval was required for this research as it did not involve human tissue or any other parts of living organisms.

References

1. Luo, J., Liu, M., Ma, L.: Origin of friction and the new frictionless technology—Superlubricity: Advancements and future outlook. Nano Energy **86**, 106092 (2021). https://doi.org/10.1016/J.NANOEN.2021.106092
2. Holmberg, K., Erdemir, A.: Influence of tribology on global energy consumption, costs and emissions. Friction **5**, 263–284 (2017). https://doi.org/10.1080/17518253.2023.2185547
3. Pichler, J., Maria Eder, R., Besser, C., Pisarova, L., Dörr, N., Marchetti-Deschmann, M., Frauscher, M.: A comprehensive review of sustainable approaches for synthetic lubricant components. Green Chem. Lett. Rev. (2023). https://doi.org/10.1080/17518253.2023.2185547
4. Syahir, A.Z., Zulkifli, N.W.M., Masjuki, H.H., Kalam, M.A., Alabdulkarem, A., Gulzar, M., Khuong, L.S., Harith, M.H.: A review on bio-based lubricants and their applications. J. Clean. Prod. **168**, 997–1016 (2017). https://doi.org/10.1016/j.jclepro.2017.09.106
5. Ijaz Malik, M.A., Kalam, M.A., Mujtaba, M.A., Almomani, F.: A review of recent advances in the synthesis of environmentally friendly, sustainable, and nontoxic bio-lubricants: Recommendations for the future implementations. Environ. Technol. Innov. **32**, 103366 (2023). https://doi.org/10.1016/j.eti.2023.103366
6. Sadiq, M.I., Ghopa, W.A.W., Nuawi, M.Z., Rasani, M.R., Sabri, M.A.M.: Experimental and numerical investigation of static and dynamic characteristics of bio-oils and SAE40 in fluid film journal bearing. Materials. **15**, 3595 (2022). https://doi.org/10.3390/MA15103595
7. Biresaw, G., Adhvaryu, A., Erhan, S.Z.: Friction properties of vegetable oils. J. Am. Oil Chem. Soc. **80**, 697–704 (2003). https://doi.org/10.1007/S11746-003-0760-7/METRICS
8. Adhvaryu, A., Erhan, S.Z., Perez, J.M.: Tribological studies of thermally and chemically modified vegetable oils for use as environmentally friendly lubricants. Wear **257**, 359–367 (2004). https://doi.org/10.1016/J.WEAR.2004.01.005
9. Reeves, C.J., Menezes, P.L., Jen, T.C., Lovell, M.R.: The influence of fatty acids on tribological and thermal properties of natural oils as sustainable biolubricants. Tribol. Int. **90**, 123–134 (2015). https://doi.org/10.1016/j.triboint.2015.04.021
10. Gul, M., Masjuki, H.H., Kalam, M.A., Zulkifli, N.W.M., Mujtaba, M.A.: A review: Role of fatty acids composition in characterizing potential feedstock for sustainable green lubricants by advance transesterification process and its global as well as Pakistani prospective. Bioenerg. Res. **13**, 1–22 (2020)
11. Hernández-Sierra, M.T., Aguilera-Camacho, L.D., Báez-García, J.E., García-Miranda, J.S., Moreno, K.J.: Thermal stability and lubrication properties of biodegradable castor oil on AISI 4140 steel. Metals **8**, 428 (2018). https://doi.org/10.3390/MET8060428
12. Saxena, A., Kumar, D., Tandon, N., Kaur, T., Singh, N.: Development of vegetable oil-based greases for extreme pressure applications: An integration of non-toxic, eco-friendly ingredients for enhanced performance. Tribol. Lett. **70**, 108 (2022). https://doi.org/10.1007/s11249-022-01651-x
13. Cecilia, J.A., Ballesteros Plata, D., Alves Saboya, R.M., de Luna, F.M., Cavalcante, C.L., Rodríguez-Castellón, E.: An overview of the biolubricant production process: Challenges and future perspectives. Processes. **8**, 257 (2020). https://doi.org/10.3390/pr8030257
14. Sánchez, R., Fiedler, M., Kuhn, E., Franco, J.M.: Tribological characterization of green lubricating greases formulated with castor oil and different biogenic thickener agents: A comparative experimental study. Ind. Lubrication Tribol. **63**, 446–452 (2011). https://doi.org/10.1108/00368791111169034/FULL/PDF
15. Acar, N., Franco, J.M., Kuhn, E., Gonçalves, D.E.P., Seabra, J.H.O.: Tribological investigation on the friction and wear behaviors of biogenic lubricating greases in steel-steel contact. Appl. Sci. **10**, 1477 (2020). https://doi.org/10.3390/app10041477
16. Sánchez, R., Franco, J.M., Delgado, M.A., Valencia, C., Gallegos, C.: Rheology of oleogels based on sorbitan and glyceryl monostearates and vegetable oils for lubricating applications. Grasas Aceites **62**, 328–336 (2011). https://doi.org/10.3989/gya.113410
17. Zhang, R., Zhang, Y., Yu, J., Gao, Y., Mao, L.: Rheology and tribology of ethylcellulose-based oleogels and W/O Emulsions as fat substitutes: Role of glycerol monostearate. Foods. **11**, 2364 (2022). https://doi.org/10.3390/FOODS11152364
18. Saxena, A., Kumar, D., Tandon, N.: Development of eco-friendly nano-greases based on vegetable oil: An exploration of the character via structure. Ind. Crops Prod. **172**, 114033 (2021). https://doi.org/10.1016/j.indcrop.2021.114033
19. Acar, N., Kuhn, E., Franco, J.M.: Tribological and rheological characterization of new completely biogenic lubricating greases: A comparative experimental investigation. Lubricants. **6**, 45 (2018). https://doi.org/10.3390/LUBRICANTS6020045
20. Vafaei, S., Jopen, M., Jacobs, G., König, F., Weberskirch, R.: Synthesis and tribological behavior of bio-based lubrication greases with bio-based polyester thickener systems. J. Clean. Prod. **364**, 132659 (2022). https://doi.org/10.1016/J.JCLEPRO.2022.132659
21. Martin, J.M., Ohmae, N.: Colloidal lubrication: General principles. In: Nanolubricants, pp. 1–13. Wiley (2008)

22. Deepika: Nanotechnology implications for high performance lubricants. SN Appl. Sci. **2**, 1–12 (2020). https://doi.org/10.1007/S42452-020-2916-8/FIGURES/5
23. Zhao, J., Huang, Y., He, Y., Shi, Y.: Nanolubricant additives: A review. Friction. **9**, 891–917 (2021). https://doi.org/10.1007/s40544-020-0450-8
24. Lee, C.T., Lee, M.B., Mong, G.R., Chong, W.W.F.: A bibliometric analysis on the tribological and physicochemical properties of vegetable oil–based bio-lubricants (2010–2021). Environ. Sci. Pollut. Res. **29**, 56215–56248 (2022). https://doi.org/10.1007/S11356-022-19746-2
25. Saleh, T.A.: Nanomaterials: classification, properties, and environmental toxicities. Environ. Technol. Innov. **20**, 101067 (2020). https://doi.org/10.1016/J.ETI.2020.101067
26. Padgurskas, J., Rukuiza, R., Prosyčevas, I., Kreivaitis, R.: Tribological properties of lubricant additives of Fe, Cu and Co nanoparticles. Tribol. Int. **60**, 224–232 (2013). https://doi.org/10.1016/J.TRIBOINT.2012.10.024
27. Wu, Y.Y., Tsui, W.C., Liu, T.C.: Experimental analysis of tribological properties of lubricating oils with nanoparticle additives. Wear **262**, 819–825 (2007). https://doi.org/10.1016/J.WEAR.2006.08.021
28. Mohamed, A., Tirth, V., Kamel, B.M.: Tribological characterization and rheology of hybrid calcium grease with graphene nanosheets and multi-walled carbon nanotubes as additives. J. Market. Res. **9**, 6178–6185 (2020). https://doi.org/10.1016/J.JMRT.2020.04.020
29. Rahman, M.M., Islam, M., Roy, R., Younis, H., AlNahyan, M., Younes, H.: Carbon nanomaterial-based lubricants: Review of recent developments. Lubricants. **10**, 281 (2022). https://doi.org/10.3390/lubricants10110281
30. Mohamed, A., Osman, T.A., Khattab, A., Zaki, M.: Tribological behavior of carbon nanotubes as an additive on lithium grease. J. Tribol. (2014). https://doi.org/10.1115/1.4028225
31. Kamel, B.M., Mohamed, A., El Sherbiny, M., Abed, K.A.: Rheology and thermal conductivity of calcium grease containing multi-walled carbon nanotube. Fullerenes Nanotubes Carbon Nanostruct. **24**, 260–265 (2016). https://doi.org/10.1080/1536383X.2016.1143462
32. Nassef, M.G.A., Hassan, H.S., Nassef, G.A., Nassef, B.G., Soliman, M., Elkady, M.F.: Activated carbon nano-particles from recycled polymers waste as a novel nano-additive to grease lubrication. Lubricants. **10**, 214 (2022). https://doi.org/10.3390/LUBRICANTS10090214
33. Nassef, M.G.A., Soliman, M., Nassef, B.G., Daha, M.A., Nassef, G.A.: Impact of graphene nano-additives to lithium grease on the dynamic and tribological behavior of rolling bearings. Lubricants. **10**, 29 (2022). https://doi.org/10.3390/lubricants10020029
34. Syed, A.: Chapter 4—oxidative stability and shelf life of vegetable oils. In: Hu, M., Jacobsen, C. (eds.) Oxidative Stability and Shelf Life of Foods Containing Oils and Fats, pp. 187–207. AOCS Press (2016)
35. Selecting the right grease for rolling bearings. World Pumps. **2015**, 31–33 (2015). https://doi.org/10.1016/S0262-1762(15)30239-X
36. Abdul Hakim Shaah, M., Hossain, Md.S., Salem Allafi, F.A., Alsaedi, A., Ismail, N., Ab Kadir, M.O., Ahmad, M.I.: A review on non-edible oil as a potential feedstock for biodiesel: Physicochemical properties and production technologies. RSC Adv. **11**, 25018–25037 (2021). https://doi.org/10.1039/D1RA04311K
37. Pradhan, D., Mishra, A.K.: Analysis of ISO VG 68 bearing oil for condition monitoring collected from an externally pressurized ball bearing system. Mater Today Proc. **44**, 4602–4606 (2021). https://doi.org/10.1016/j.matpr.2020.10.831
38. Hannon, W.M., Ai, X.: Rolling bearing lubricants. In: Encyclopedia of Tribology, pp. 2848–2856. Springer, Boston (2013)
39. Mubofu, E.B.: Castor oil as a potential renewable resource for the production of functional materials. Sustain. Chem. Process. **4**, 1–12 (2016). https://doi.org/10.1186/S40508-016-0055-8
40. Yeboah, A., Ying, S., Lu, J., Xie, Y., Amoanimaa-Dede, H., Boateng, K.G.A., Chen, M., Yin, X.: Castor oil (Ricinus communis): A review on the chemical composition and physicochemical properties. Food Sci. Technol. **41**, 399–413 (2021). https://doi.org/10.1590/fst.19620
41. Sánchez, M., Avhad, M.R., Marchetti, J.M., Martínez, M., Aracil, J.: Jojoba oil: A state of the art review and future prospects. Energy Convers Manag. **129**, 293–304 (2016). https://doi.org/10.1016/J.ENCONMAN.2016.10.038
42. Matsumoto, Y., Ma, S., Tominaga, T., Yokoyama, K., Kitatani, K., Horikawa, K., Suzuki, K.: acute effects of transdermal administration of jojoba oil on lipid metabolism in mice. Medicina **55**, 594 (2019). https://doi.org/10.3390/MEDICINA55090594
43. Özcan, M.M., Ünver, A., Erkan, E., Arslan, D.: Characteristics of some almond kernel and oils. Sci. Hortic. **127**, 330–333 (2011). https://doi.org/10.1016/J.SCIENTA.2010.10.027
44. Thommes, M., Kaneko, K., Neimark, A.V., Olivier, J.P., Rodriguez-Reinoso, F., Rouquerol, J., Sing, K.S.W.: Physisorption of gases, with special reference to the evaluation of surface area and pore size distribution (IUPAC technical report). Pure Appl. Chem. **87**, 1051–1069 (2015). https://doi.org/10.1515/pac-2014-1117
45. Li, W., Yang, K., Peng, J., Zhang, L., Guo, S., Xia, H.: Effects of carbonization temperatures on characteristics of porosity in coconut shell chars and activated carbons derived from carbonized coconut shell chars. Ind. Crops Prod. **28**, 190–198 (2008). https://doi.org/10.1016/J.INDCROP.2008.02.012
46. Pol, V.G.: Upcycling: Converting waste plastics into paramagnetic, conducting, solid, pure carbon microspheres. Environ. Sci. Technol. **44**, 4753–4759 (2010). https://doi.org/10.1021/es100243u
47. El Essawy, N.A., Ali, S.M., Farag, H.A., Konsowa, A.H., Elnouby, M., Hamad, H.A.: Green synthesis of graphene from recycled PET bottle wastes for use in the adsorption of dyes in aqueous solution. Ecotoxicol. Environ. Saf. **145**, 57–68 (2017). https://doi.org/10.1016/J.ECOENV.2017.07.014
48. Parra, J.B., Ania, C.O., Arenillas, A., Rubiera, F., Pis, J.J., Palacios, J.M.: Structural changes in polyethylene terephthalate (PET) waste materials caused by pyrolysis and CO2 activation. Adsorpt. Sci. Technol. **24**, 439–450 (2006). https://doi.org/10.1260/026361706779849735
49. Bratek, W., Świątkowski, A., Pakuła, M., Biniak, S., Bystrzejewski, M., Szmigielski, R.: Characteristics of activated carbon prepared from waste PET by carbon dioxide activation. J. Anal. Appl. Pyrolysis **100**, 192–198 (2013). https://doi.org/10.1016/J.JAAP.2012.12.021
50. Pimenta, M.A., Dresselhaus, G., Dresselhaus, M.S., Cançado, L.G., Jorio, A., Saito, R.: Studying disorder in graphite-based systems by Raman spectroscopy. Phys. Chem. Chem. Phys. **9**, 1276–1290 (2007). https://doi.org/10.1039/B613962K
51. Lian, F., Xing, B., Zhu, L.: Comparative study on composition, structure, and adsorption behavior of activated carbons derived from different synthetic waste polymers. J. Colloid Interface Sci. **360**, 725–730 (2011). https://doi.org/10.1016/j.jcis.2011.04.103
52. Esfandiari, A., Kaghazchi, T., Soleimani, M.: Preparation and evaluation of activated carbons obtained by physical activation of polyethyleneterephthalate (PET) wastes. J. Taiwan Inst. Chem. Eng. **43**, 631–637 (2012). https://doi.org/10.1016/J.JTICE.2012.02.002

53. Ji, Z., Shen, X., Song, Y., Zhu, G.: In situ synthesis of graphene/cobalt nanocomposites and their magnetic properties. Mater. Sci. Eng. B **176**, 711–715 (2011). https://doi.org/10.1016/J.MSEB.2011.02.026
54. Chauke, N.P., Mukaya, H.E., Nkazi, D.B.: Chemical modifications of castor oil: A review. Sci. Prog. **102**, 199–217 (2019). https://doi.org/10.1177/0036850419859118
55. Van Boven, M., Holser, R.A., Cokelaere, M., Decuypere, E., Govaerts, C., Lemey, J.: Characterization of triglycerides isolated from jojoba oil. J. Am. Oil Chem. Soc. **77**, 1325–1329 (2000). https://doi.org/10.1007/s11746-000-0207-1
56. Al Ghamdi, A.K., Elkholy, T.A., Abuhelal, S., Alabbadi, H., Qahwaji, D., Sobhy, H., Khalefah, N., Hilal, M.A.: Study of jojoba (Simmondsia chinensis) oil by gas chromatography. Nat. Prod. Chem. Res. **5**, 282 (2017). https://doi.org/10.4172/2329-6836.1000283
57. Bouhadi, N., Chennit, B., Chebrouk, F., Boudriche, L.: Physicochemical characteristics, phenol content and fatty acids of bitter almond oil. Arch. Ecotoxicol. **3**, 118–124 (2021). https://doi.org/10.36547/ae.2021.3.4.118-124
58. Mohammed Hassan Jabal, A.R.A., Abd, H.S.: Experimental investigation of tribological characteristics and emissions with nonedible sunflower oil as a biolubricant. J Air Waste Manage Assoc. **69**, 109–118 (2019). https://doi.org/10.1080/10962247.2018.1523070
59. Esteban, B., Riba, J.R., Baquero, G., Puig, R., Rius, A.: Characterization of the surface tension of vegetable oils to be used as fuel in diesel engines. Fuel **102**, 231–238 (2012). https://doi.org/10.1016/J.FUEL.2012.07.042
60. Shu, Q., Wang, J., Peng, B., Wang, D., Wang, G.: Predicting the surface tension of biodiesel fuels by a mixture topological index method, at 313 K. Fuel **87**, 3586–3590 (2008). https://doi.org/10.1016/J.FUEL.2008.07.007
61. Rizza, M.A., Wijayanti, W., Hamidi, N., Wardana, I.N.G.: Role of intermolecular forces on the contact angle of vegetable oil droplets during the cooling process. Sci. World J. **2018**, 5283753 (2018). https://doi.org/10.1155/2018/5283753
62. Seid Ahmed, Y., González, L.W.H.: Ti6Al4V grinding using different lubrication modes for minimizing energy consumption. Int. J. Adv. Manuf. Technol. **126**, 2387–2405 (2023). https://doi.org/10.1007/s00170-023-11203-9
63. Nassef, B.G., Pape, F., Poll, G.: Enhancing the performance of rapeseed oil lubricant for machinery component applications through hybrid blends of nanoadditives. Lubricants. **11**, 479 (2023). https://doi.org/10.3390/lubricants11110479
64. Darminesh, S.P., Sidik, N.A.C., Najafi, G., Mamat, R., Ken, T.L., Asako, Y.: Recent development on biodegradable nanolubricant: A review. Int. Commun. Heat Mass Transfer **86**, 159–165 (2017). https://doi.org/10.1016/j.icheatmasstransfer.2017.05.022
65. Amiruddin, H., Bin Abdollah, M.F., Mohamad Norani, M.N.: Lubricity and mechanical stability of bio-grease formulated from non-edible vegetable oil. Proc. Inst. Mech. Eng. Part J: J. Eng. Tribol. **237**, 589–600 (2022). https://doi.org/10.1177/13506501221121904
66. Borrero-López, A.M., Valencia, C., Blánquez, A., Hernández, M., Eugenio, M.E., Franco, J.M.: Cellulose pulp- and castor oil-based polyurethanes for lubricating applications: Influence of streptomyces action on barley and wheat straws. Polymers **12**, 2822 (2020). https://doi.org/10.3390/polym12122822
67. Gallego, R., Cidade, T., Sánchez, R., Valencia, C., Franco, J.M.: Tribological behaviour of novel chemically modified biopolymer-thickened lubricating greases investigated in a steel–steel rotating ball-on-three plates tribology cell. Tribol. Int. **94**, 652–660 (2016). https://doi.org/10.1016/j.triboint.2015.10.028
68. Sharma, A., Amarnath, M., Kankar, P.K.: Novel ensemble techniques for classification of rolling element bearing faults. J. Braz. Soc. Mech. Sci. Eng. **39**, 709–724 (2017). https://doi.org/10.1007/s40430-016-0540-8
69. Yakout, M., Elkhatib, A., Nassef, M.G.A.: Rolling element bearings absolute life prediction using modal analysis. J. Mech. Sci. Technol. **32**, 91–99 (2018). https://doi.org/10.1007/s12206-017-1210-1
70. Maru, M.M., Castillo, R.S., Padovese, L.R.: Study of solid contamination in ball bearings through vibration and wear analyses. Tribol. Int. **40**, 433–440 (2007). https://doi.org/10.1016/J.TRIBOINT.2006.04.007
71. Wu, C., Hong, Y., Ni, J., Teal, P.D., Yao, L., Li, X.: Investigation of mixed hBN/Al2O3 nanoparticles as additives on grease performance in rolling bearing under limited lubricant supply. Colloids Surf A Physicochem Eng Asp **659**, 130811 (2023). https://doi.org/10.1016/j.colsurfa.2022.130811
72. Kireitseu, M., Hui, D., Tomlinson, G.: Advanced shock-resistant and vibration damping of nanoparticle-reinforced composite material. Compos. B Eng. **39**, 128–138 (2008). https://doi.org/10.1016/j.compositesb.2007.03.004
73. Singh, R.K., Dixit, A.R., Sharma, A.K., Tiwari, A.K., Mandal, V., Pramanik, A.: Influence of graphene and multi-walled carbon nanotube additives on tribological behaviour of lubricants. Int. J. Surf. Sci. Eng. **12**, 207–227 (2018). https://doi.org/10.1504/IJSURFSE.2018.094773
74. Ju, C., Li, W., Zhao, Q., Wang, X.: Bio-additives derived from ricinoleic acid and choline with improved tribological properties in lithium base grease. J. Oleo Sci. **71**, 915–925 (2022). https://doi.org/10.5650/jos.ess21435
75. Deivajothi, P., Manieniyan, V., Sivaprakasam, S.: Experimental investigation on DI diesel engine with fatty acid oil from by-product of vegetable oil refinery. Ain Shams Eng. J. **10**, 77–82 (2019). https://doi.org/10.1016/j.asej.2018.04.005
76. Singh, A.K.: Castor oil-based lubricant reduces smoke emission in two-stroke engines. Ind. Crops Prod. **33**, 287–295 (2011). https://doi.org/10.1016/J.INDCROP.2010.12.014
77. Syahrullail, S., Kamitani, S., Shakirin, A.: Performance of vegetable oil as lubricant in extreme pressure condition. Procedia Eng. **68**, 172–177 (2013). https://doi.org/10.1016/j.proeng.2013.12.164
78. Arnšek, A., Vižintin, J.: Lubricating properties of rapeseed-based oils. J. Synth. Lubrication **16**, 281–296 (2000). https://doi.org/10.1002/jsl.3000160402
79. Çalhan, R., Kaskun Ergani, S., Uslu, S.: Synthesis of Fe–Ni–TiO_2/activated carbon nanoparticles and evaluation of catalytic activity in a palm oil/diesel fuel blended diesel engine and optimization with RSM. Sci. Technol. Energy Transition **78**, 16 (2023). https://doi.org/10.2516/stet/2023013
80. Ji, L., Chen, W., Duan, L., Zhu, D.: Mechanisms for strong adsorption of tetracycline to carbon nanotubes: A comparative study using activated carbon and graphite as adsorbents. Environ. Sci. Technol. **43**, 2322–2327 (2009). https://doi.org/10.1021/es803268b
81. Waara, P., Hannu, J., Norrby, T., Byheden, Å.: Additive influence on wear and friction performance of environmentally adapted lubricants. Tribol. Int. **34**, 547–556 (2001). https://doi.org/10.1016/S0301-679X(01)00045-7
82. Stachowiak, G.W., Batchelor, A.W.: Engineering Tribology, 4th edn. Elsevier Inc (2013)
83. Vencl, A., Gašić, V., Stojanović, B.: Fault tree analysis of most common rolling bearing tribological failures. IOP Conf Ser Mater Sci Eng. **174**, 12048 (2017). https://doi.org/10.1088/1757-899X/174/1/012048
84. Bearing damage analysis | Evolution. https://evolution.skf.com/bearing-damage-analysis-iso-15243-is-here-to-help-you/

85. Harris, T.A.: Rolling Bearing Analysis. Wiley (2001)
86. Howard, I.: A review of rolling element bearing vibration "Detection, Diagnosis and Prognosis." (1994)
87. Berry, J.E.: How to track rolling element bearing health with vibration signature analysis. Sound Vibration. **25**, 24–35 (1991)
88. Jakubek, B., Barczewski, R.: The influence of kinematic viscosity of a lubricant on broadband rolling bearing vibrations in amplitude terms. Diagnostyka **20**, 93–102 (2019). https://doi.org/10.29354/diag/100440
89. Serrato, R., Maru, M.M., Padovese, L.R.: Effect of lubricant viscosity grade on mechanical vibration of roller bearings. Tribol. Int. **40**, 1270–1275 (2007). https://doi.org/10.1016/j.triboint.2007.01.025
90. Su, Y.-T., Sheen, Y.-T., Lin, M.-H.: Signature analysis of roller bearing vibrations: lubrication effects. Proc. Inst. Mech. Eng. C J. Mech. Eng. Sci. **206**, 193–202 (1992). https://doi.org/10.1243/PIME_PROC_1992_206_115_02
91. Hamrock, B.J., Dowson, D.: Isothermal elastohydrodynamic lubrication of point contacts: Part III—fully flooded results. J. Lubr. Technol. **99**, 264–275 (1977). https://doi.org/10.1115/1.3453074
92. Cen, H., Lugt, P.M., Morales-Espejel, G.: On the film thickness of grease-lubricated contacts at low speeds. Tribol. Trans. **57**, 668–678 (2014). https://doi.org/10.1080/10402004.2014.897781
93. Cen, H., Lugt, P.M., Morales-Espejel, G.: Film thickness of mechanically worked lubricating grease at very low speeds. Tribol. Trans. **57**, 1066–1071 (2014). https://doi.org/10.1080/10402004.2014.933936
94. Cen, H., Lugt, P.M.: Film thickness in a grease lubricated ball bearing. Tribol. Int. **134**, 26–35 (2019). https://doi.org/10.1016/j.triboint.2019.01.032
95. Schmit, J., Han, S., Novak, E.: Ball bearing measurement with white light interferometry. In: Lehmann, P.H. (ed.) Optical Measurement Systems for Industrial Inspection VI, p. 73890P. SPIE (2009)